Published in final edited form as:

J Neuroophthalmol. 2022 December 01; 42(4): 442–453. doi:10.1097/WNO.0000000000001717.

* *Corresponding author:* Laura Balcer, MD, MSCE, Department of Neurology, NYU School of Medicine, 222 E. 41st St. New York, NY 10017, Tel. +646 501 7861, Fax: +212 263 7721, laura.balcer@nyulangone.org.

Disclosure Statements:

Laura Balcer is editor-in-chief of the *Journal of Neuro-Ophthalmology*.

Alexander U. Brandt is named as inventor on several patents and patent applications describing multiple sclerosis serum biomarkers, retinal image analysis methods and human pose estimation methods. He is cofounder and holds shares in companies Motognosis and Nocturne.

Peter A. Calabresi is PI on grants to Johns Hopkins from Principia and Genentech. He has consulted for Disarm, Nerveda, Biogen and Avidea.

Elliot Frohman has received consulting and speaker fees from Novartis, Genzyme, Biogen, Alexion, and Janssen.

Teresa Frohman has received consulting fees from Alexion

Steven Galetta has been a consultant for Biogen and Genentech.

Joachim Havla reports grants for OCT research from the Friedrich-Baur-Stiftung and Merck, personal fees and non-financial support from Celgene, Merck, Alexion, Novartis, Roche, Santhera, Biogen, Heidelberg Engineering, Sanofi Genzyme and non-financial support of the Guthy-Jackson Charitable Foundation, all outside the submitted work.

Bernhard Hemmer has served on scientific advisory boards for Novartis; he has served as DMSC member for AllergyCare, Polpharma and TG therapeutics; he or his institution have received speaker honoraria from Desitin; His institution received research grants from Regeneron for MS research. He holds part of two patents; one for the detection of antibodies against KIR4.1 in a subpopulation of patients with MS and one for genetic determinants of neutralizing antibodies to interferon. All conflicts are not relevant to the topic of the study.

Benjamin Knier received travel support and a research grant from Novartis (Oppenheim research award).

Friedemann Paul serves as an Associate Editor for *Neurology: Neuroimmunology & Neuroinflammation*, reports research grants and speaker honoraria from Bayer, Teva, Genzyme, Merck, Novartis, MedImmune and is member of the steering committee of the OCTIMS study (Novartis).

Athina Papadopoulou has received speaker-fee from Sanofi-Genzyme and travel support from Bayer AG, Teva and Hoffmann-La Roche. Her research was/is being supported by the University and University Hospital of Basel, the Swiss Multiple Sclerosis Society, the “Stiftung zur Förderung der gastroenterologischen und allgemeinen klinischen Forschung sowie der medizinischen Bildauswertung” and the Swiss National Science Foundation (Project number: P300PB_174480)

Axel Petzold is supported by the National Institute for Health Research (NIHR) Biomedical Research Centre based at Moorfields Eye Hospital NHS Foundation Trust and UCL Institute of Ophthalmology. AP is part of the steering committee of the ANGI network which is sponsored by ZEISS, steering committee of the OCTiMS study which is sponsored by Novartis and reports speaker fees from Heidelberg-Engineering.

Shiv Saidha has received consulting fees from Medical Logix for the development of CME programs in neurology and has served on scientific advisory boards for Biogen, Genzyme, Genentech Corporation, EMD Serono & Celgene. He has consulted for Carl Zeiss Meditec. He is the PI of investigator-initiated studies funded by Genentech Corporation and Biogen Idec, and received support from the Race to Erase MS foundation. He has received equity compensation for consulting from JuneBrain LLC, a retinal imaging device developer.

Joel S. Schuman

Aerie Pharmaceuticals, Inc.: Consultant/Advisor, Equity Owner

BrightFocus Foundation: Grant Support

Boehringer Ingelheim: Consultant/Advisor

Carl Zeiss Meditec: Patents/Royalty/Consultant/Advisor

Massachusetts Eye and Ear Infirmary and Massachusetts Institute of Technology: Intellectual Property

National Eye Institute: Grant Support

New York University: Intellectual Property

Ocugenix: Equity Owner, Patents/Royalty

Ocular Therapeutix, Inc.: Consultant/Advisor, Equity Owner

Opticient: Consultant/Advisor, Equity Owner

Perfuse, Inc.: Consultant/Advisor

Regeneron, Inc.: Consultant/Advisor

SLACK Incorporated: Consultant/Advisor

Tufts University: Intellectual property

University of Pittsburgh: Intellectual property

Pablo Villoslada holds stocks and have received consultancy fees from Accure therapeutics, Spiral Therapeutics, QMENTA, Attune Neurosciences, CLight, NeuroPrex and Adhera Health.

Hanna G. Zimmermann received research grants from Novartis and speaking honoraria from Bayer Healthcare.

The remaining authors report no disclosures.

Peter A. Calabresi is supported by R01NS082347.

Joachim Havla is (partially) funded by the German Federal Ministry of Education and Research (Grant Numbers 01ZZ1603[A-D] and 01ZZ1804[A-H] (DIFUTURE)).

Normative Data and Conversion Equation for Spectral-Domain Optical Coherence Tomography in an International Healthy Control Cohort

Rachel Kenney, PhD[1,2], **Mengling Liu, PhD**[2], **Lisena Hasanaj, MPA**[1], **Binu Joseph, MBBS**[1], **Abdullah Abu Al-Hassan, MD**[3], **Lisanne Balk, PhD**[4], **Raed Behbehani, MD**[3], **Alexander U. Brandt, MD**[5,6], **Peter A. Calabresi, MD**[7], **Elliot M. Frohman, MD, PhD**[8], **Teresa Frohman, PA-C**[8], **Joachim Havla, MD**[9,10], **Bernhard Hemmer, MD**[11,12], **Hong Jiang, MD**[13], **Benjamin Knier, MD**[11], **Thomas Korn, MD**[11,12], **Letizia Leocani, MD**[14], **Elena H. Martínez-Lapiscina, MD, PhD**[15], **Athina Papadopoulou, MD**[5,16], **Friedemann Paul, MD**[5,17], **Axel Petzold, MD, PhD**[18], **Marco Pisa, MD**[14], **Pablo Villoslada, MD**[15], **Hanna Zimmermann, M.Eng**[5,17], **Hiroshi Ishikawa, MD**[19], **Joel S. Schuman, MD**[20,21,22,23], **Gadi Wollstein, MD**[20], **Yu Chen, MPH, PhD**[2], **Shiv Saidha, MBBCh, MD, MRCPI**[7], **Lorna E. Thorpe, MPH, PhD**[2], **Steven L. Galetta, MD**[1,20], **Laura J. Balcer, MD, MSCE**[1,2,20] **IMSVISUAL Consortium**

[1-]Department of Neurology, New York University Grossman School of Medicine, New York, NY, USA

[2-]Department of Population Health, New York University Grossman School of Medicine, New York, NY, USA

[3-]Al-Bahar Ophthalmology Center, Ibn Sina Hospital, Kuwait City, Kuwait

[4-]Mulier Institute, Centre for Research on Sports in Society, Utrecht, Netherlands

Bernhard Hemmer received funding for the study by the European Union's Horizon 2020 Research and Innovation Program (grant MultipleMS, EU RIA 733161) and the Deutsche Forschungsgemeinschaft (DFG, German Research Foundation) under Germany's Excellence Strategy within the framework of the Munich Cluster for Systems Neurology (EXC 2145 SyNergy – ID 390857198)
Benjamin Knier is funded by the Else Kröner-Fresenius-Stiftung (Else Kröner-Fresenius Exzellenzstipendium).
Thomas Korn is funded by the DFG (SFB1054-B06, TRR128-A07, TRR128-A12, TRR274-A01, Synergy Cluster of Excellence, EXC 2145, ID 390857198) and by the ERC (CoG 647215)
Joel S. Schuman received funding from the National Institutes of Health (Bethesda, MD, USA) R01-EY013178. An unrestricted grant from Research to Prevent Blindness (New York, NY) to the Department of Ophthalmology, NYU Langone Health, NYU Grossman School of Medicine, New York, NY.
Pablo Villoslada is funded by Instituto de Salud Carlos III, Spain and Fondo Europeo de Desarrollo Regional (PI15/0061)
Statement of Authorship
-Conception and design:
All authors
-Acquisition of data:
All authors
-Analysis and interpretation of data:
Laura Balcer
Rachel Kenney
-Drafting the manuscript:
Rachel Kenney
Laura Balcer
-Revising the manuscript for intellectual content:
All authors
-Final approval of the completed manuscript:
All authors

[5]Experimental and Clinical Research Center, Max Delbrueck Center for Molecular Medicine and Charité – Universitätsmedizin Berlin, corporate member of Freie Universität Berlin and Humboldt-Universität zu Berlin, Berlin, Germany

[6]Department of Neurology, University of California, Irvine, CA, USA

[7]Department of Neurology, Johns Hopkins University, Baltimore, MD, USA

[8]Laboratory of Neuroimmunology, of Professor Lawrence Steinman, Stanford University School of Medicine, Palo Alto, CA, USA

[9]Institute of Clinical Neuroimmunology, LMU Hospital,, Ludwig Maximilians Universität München, Munich, Germany

[10]Data Integration for Future Medicine consortium (DIFUTURE), Ludwig-Maximilians University, Munich, Germany

[11]Department of Neurology, Klinikum rechts der Isar, School of Medicine, Technical University of Munich, Munich, Germany

[12]Munich Cluster for Systems Neurology (SyNergy), Munich, Germany

[13]Bascom Palmer Eye Institute, Department of Neurology, University of Miami Miller School of Medicine, Miami, FL, USA

[14]Vita-Salute University & Hospital San Raffaele, Milano, Italy

[15]Center of Neuroimmunology and Department of Neurology, Hospital Clinic of Barcelona, Institut d'Investigacions Biomèdiques August Pi Sunyer (IDIBAPS), University of Barcelona, Villarroel 170, Barcelona ES 08036, Spain.

[16]Neurologic Clinic and Policlinic, MS Center and Research Center for Clinical Neuroimmunology and Neuroscience (RCN2NB) Basel, University Hospital Basel and University of Basel, Basel, Switzerland

[17]NeuroCure Clinical Research Center, Charité – Universitätsmedizin Berlin, corporate member of Freie Universität Berlin and Humboldt-Universität zu Berlin, Berlin, Germany

[18]Moorfields Eye Hospital, City Road, London; The National Hospital for Neurology and Neurosurgery, Queen Square, UCL Institute of Neurology, London, United Kingdom; Dutch Neuro-ophthalmology Expertise Centre, Amsterdam UMC, The Netherlands

[19]Oregon Health and Science University, Portland, OR, USA

[20]Department of Ophthalmology, New York University Grossman School of Medicine, New York, NY, USA

[21]Departments of Biomedical Engineering and Electrical and Computer Engineering, New York University Tandon School of Engineering, Brooklyn, NY, USA

[22]Center for Neural Science, NYU, New York, NY, USA

[23]Neuroscience Institute, NYU Langone Health, New York, NY, USA.

Keywords

IMSVISUAL; Spectral-Domain Optical Coherence Tomography; Peripapillary Retinal Nerve Fiber Layer; Ganglion Cell + Inner Plexiform Layer; Normative Database

In neurology, OCT has become an important method to determine in integrity of visual pathway. One example is MS, with OCT studies for over 10 years. As more studies have been published describing the association of SD-OCT measurements with brain atrophy and with reductions in visual function test scores, the use of OCT as a structural outcome measure in clinical trials of MS therapies is more widely adopted(1). With collaborations of neuro-ophthalmologists and MS specialists, the use of multiple OCT devices has created challenges for synergizing sites for trials. Often, clinical trials will use one or both of the two most common SD-OCT platforms (Cirrus HD-OCT or Spectralis); however, individual pRNFL and GCIPL thickness measurements are not interchangeable between these devices(2–5) unless consistent segmentation algorithms are used or the sample size is large enough to overcome systematic differences. SD-OCT measurements have high levels of reproducibility and low degrees of variability within each of the SD-OCT platforms for healthy controls(6) and in MS participants(7, 8) across multi-center studies(9). Measurements from the Cirrus and Spectralis SD-OCT devices are often pooled together despite differences in software algorithms, hardware/optical components and segmentation areas(3, 10).

Equations that convert pRNFL and GCIPL measurement between the two most widely used SD-OCT devices will be useful for clinical trials, clinical practice and for observational studies. Such an equation will provide a method to relate measurements obtained by Spectralis and Cirrus SD-OCT platforms and to more accurately pool data. Previous investigations have estimated conversion equations for pRNFL thickness in healthy volunteers and in participants with glaucoma(3, 11). The relation between GCIPL measurements for the Cirrus vs. Spectralis OCT platforms has not been investigated.

Normative data is important to provide a basis to compare to retinal degeneration seen in MS. The availability of normative data for spectral-domain (SD-) optical coherence tomography (OCT) measurements is currently limited by the lack of a large world-wide representative sample of normative data across age groups. Current normative values are based on the following: 1) healthy control comparison groups from published studies that may be subject to selection bias and are not stratified by age, sex, or race; 2) normative values provided in the OCT device software by the manufacturers, whose analyses were based on small sample sizes (fewer than 300 subjects in the Cirrus HD-OCT normative cohort), did not include macular scans (Spectralis normative cohort), and also do not account for the potential effects of sex, race, or ethnicity.

A number of recent studies demonstrate meaningful variability in SD-OCT measurements by age, sex and race, suggesting that these current value models are potentially problematic (12, 13). Thinner peripapillary retinal nerve fiber layer thickness (pRNFL) measurements were associated with older age and Caucasian race in a study using one of the first versions of OCT technology (time-domain) (14). A study of people with multiple sclerosis (MS) by

Kimbrough et al. (ref) showed that African Americans (AA) had higher baseline pRNFL thicknesses in the healthy control group compared to non- AA individuals. However, there were no differences in GCIPL values at baseline between AA participants and non-AA individuals in the healthy control group(15). This study had a small sample size (n=14 AA healthy controls). Another study with 31 AAs and 61 Caucasians found higher pRNFL values in the AA group, with no differences in GCIPL thickness between groups(16). Larger international studies that evaluate the effects of age, sex, and race/ethnicity on SD-OCT pRNFL and GCIPL measurements in healthy controls are needed to provide normative values that represent various ages, sex, and demographic subgroups.

The purpose of this investigation was to develop a conversion equation for pRNFL and GCIPL thicknesses to improve comparability of these measurements derived from the Cirrus HD-OCT and Spectralis OCT devices in healthy controls. We also sought examine the effect of age, sex, and race/ethnicity on OCT measurements in a large international cohort of healthy control participants.

Methods:

Study Cohort:

OCT and high-contrast visual acuity measurements were collected for 546 healthy controls. Participants were ≥18 years of age with no history of ocular or neurological disease; high-contrast visual acuities were better than 20/40, and refractive error was between −6 and +6 spherical diopters, inclusive. Participants were part of an 11-site collaboration within the IMSVISUAL (International MS Visual System) consortium in the United States, Europe, and the Middle East. IMSVISUAL is an international, collaborative group of researchers with over 140 members from 40 countries that investigate the visual pathway in MS and related demyelinating disorders (www.imsvisual.org)(17). Through concerted collaborative efforts, IMSVISUAL has facilitated high-quality, large-scale studies of the visual system in MS, including those examining the association of OCT measurements with future MS disability(18). IMSVIUSAL has established guidelines for reporting OCT in published studies,(19, 20) and previous work from our group that established ideal inter-eye difference thresholds for utilizing OCT measurements in the diagnosis of optic nerve lesions,(21) have also been determined through a recent IMSVISUAL collaboration. For the present study, each site's institutional review board approved the study procedures. All participants provided written informed consent to participate in research studies at the individual sites. Data sharing agreements were completed between each study site and New York University (NYU) Grossman School of Medicine.

Age at time of visit was self-reported or calculated as the difference between date of birth and date of visit. Age was categorized in decades (<30, 30–39, 40–49, 50–59, 60–69, 70+). Race/ethnicity data were collected, and participants were self-categorized as Non-Hispanic Caucasian, Non-Hispanic African American, Hispanic, Asian or Pacific Islander, Alaskan or American Indian or Other. These racial and ethnicity categories are based on the United States Census guidelines. However, since very few participants self-identified as Hispanic, separating Hispanic Caucasians and Hispanic African Americans was not feasible; therefore, Hispanic was defined as its own category.

Optical Coherence Tomography (OCT).

Either Spectralis SD-OCT (Heidelberg Engineering, Heidelberg, Germany) or Cirrus HD-OCT (Carl Zeiss Meditec, Dublin, CA), or both, were performed for all participants by a trained technologist as part of ongoing MS vision research studies at all sites. Peripapillary RNFL (pRNFL) thickness was measured using a 3.4 mm peripapillary ring scan on the Spectralis OCT. On the Cirrus OCT, optic nerve head (ONH) Cube 200×200 scans were used to measure pRNFL thickness in a 3.4 mm circle centered on the optic disc.

Macular volume scans encompassing a >6 mm area surrounding the fovea were obtained using custom scans on the Spectralis OCT and by automated macular volume cube 200×200 or 512×128 (6×6mm) scans on the Cirrus OCT. Macular GCIPL thickness was measured as the sum of the ganglion cell layer plus inner plexiform layer thicknesses and was collected for healthy control participants at five of the sites in the IMSVISUAL study. GCIPL measurements were obtained using the automated macular volume cube scans with a measurement area of a 4×5 mm annulus surrounding the fovea(7) on Cirrus OCT, and from the macular volume scan encompassing a 6×6 mm cylinder surrounding the fovea on the Spectralis OCT.

Automated segmentation protocols with manual inspection and correction of lines delineating retinal layers were used for all scans. Manual review of the OCT images by trained technicians and/or clinicians was performed to ensure that all scans met quality control standards. The OSCAR-IB criteria for scan quality control(22) were followed for all OCT scans. OCT results are reported in this manuscript in concordance with the APOSTEL 2.0 guidelines(19, 20). Cirrus and Spectralis OCT data were collected on the same day for the same participants at one study site (NYU). Repeated Cirrus OCT (2 or more scans with the same protocol on the same device) and repeated Spectralis OCT measurements were also collected in a subset of participants at the NYU site.

Statistical Analyses:

Conversion Equation—Since two SD-OCT devices were used in these studies (devices chosen by study sites based on institutional preference and prior to the inception and design of these analyses), a conversion equation was developed using a structural equation model (Figure 1). This model accounted for clustering since two eyes were included for each subject; the model was based on the 173 participants (346 eyes) for pRNFL and 114 participants (228 eyes) for GCIPL thicknesses who were scanned on the same day using both OCT devices and with repeated measures on one or both devices at one site (NYU). The maximum likelihood with missing values (MLMV) method was used; this assumes joint normality of all variables and that missing values are missing at random and allows observations with missing values to be included in the model. Structural equation modeling (SEM), similar to a regression equation, provides the intercept and beta coefficient to convert between devices; however, the SEM also considers unmeasured error in the devices, and is, therefore, more accurate than using regression modeling alone(23).

Path (or regression) coefficients are a measure of association between the two devices and capture related changes between the two devices. The path coefficients were constrained to

1 and the intercepts were constrained to 0 for the Cirrus device, allowing Cirrus to be the reference device compared to Spectralis. The path coefficients for Spectralis measurements were constrained to be equal since they are inherent to the device and assumed not to vary between measures, as were the intercepts. The conversion equation was validated using leave-one-out cross validation (LOOCV) on an independent dataset of participants who had measurements on both devices on the same day, but did not have repeated measures on either device and therefore were not included in the SEM developing the conversion equation. The equation was validated in both healthy controls and people with MS separately. The independent dataset of healthy controls included 95 eyes for pRNFL and 22 eyes for GCIPL. The independent dataset of people with MS included 37 eyes for pRNFL and 6 eyes for GCIPL (which may be too small to validate results for GCIPL in people with MS). Intra-operator reproducibility for each device was evaluated by the intraclass correlation coefficient (ICC) and coefficient of variation (CV).

Once the conversion equation was developed, data were pooled together to increase sample size for further analysis since some sites used Cirrus OCT only and some sites used only Spectralis OCT measurements. Values from Cirrus device were used when those data were available, and values from Spectralis device were converted based on the conversion equation developed. This method was used to reduce systematic bias from having measurements from different devices with different image acquisition and segmentation algorithms; this also increases sample size and power of the study by allowing for pooling of data from the two OCT devices.

Normative data analysis—Inter-eye pRNFL and GCIPL differences were calculated by subtracting right eye from left eye values and using the absolute value of the difference. Descriptive statistics report continuous variables as means and standard error (SE) and categorical variables as frequency and percentages. Means and standard errors were calculated using linear mixed effects model, which account for clustering since two eyes were used for each participant. The effects of age, sex, and race/ethnicity on pRNFL and GCIPL thickness were evaluated using generalized estimating equation (GEE) regression models accounting for within-subject, inter-eye correlations since both eyes of each participant were included in the model. Bland-Altman plots were created using Stata 16.0 to compare OCT thickness values between devices.

Changepoint analyses to determine inflection points where pRNFL and GCIPL thicknesses change with respect to their degrees decline were performed with the ‘segmented’ package in R and confirmed in Python. Changepoint analysis with one inflection point evaluates the differences in slope before and after the inflection point at multiple points to determine the point where the slopes have the greatest difference. Age was also dichotomized based on results of changepoint analyses as a secondary analysis to look for differences in progression before and after the change point. Missing race data (11.5%) and GCIPL data (25.6%) were imputed using the MICE command in Stata 16.0 with 100 multiple imputations as a sensitivity analysis. Additional sensitivity analyses examining associations of SD-OCT measures with age, race/ethnicity and sex were performed for data from each OCT device to ensure that trends seen were not affected by pooling of the data. Analyses were performed using Stata 16.0, R and Python software.

Results:

Study Cohort

Data from healthy control participants (n=546) from 9 sites in the IMSVISUAL consortium were included in this study. Six healthy controls in the cohort were excluded for not having age information available, resulting in a final pooled cohort size of 540 healthy controls. The cohort had a fairly equal distribution of women and men (54% male), was primarily Caucasian (76%), and had a wide distribution of ages from ranging from 18–87, with a mean (SD) of 39.3 (14.6) years. Demographics of these participants and are shown in Table 1. Distribution of racial groups by country is shown in Supplementary Table 1. The non-US cohorts were comprised almost exclusively by Caucasians, reflecting the demographics of those countries.

Conversion Equation

At the single site (NYU) used for development of the conversion equation and OCT reproducibility results, PRNFL measurements were performed on both Cirrus and Spectralis devices on 346 healthy control eyes and GCIPL measurements were performed on 228 healthy control eyes on both Cirrus and Spectralis devices. Number of eyes with repeated scans on each device are shown in Figure 2. Eyes with poor quality scans or ocular pathology were excluded. Both Cirrus and Spectralis platforms had excellent reproducibility for both pRNFL and GCIPL measurements (ICC ranging from 0.995–0.998), although the sample size for GCIPL on the Spectralis machine was small. Reproducibility results for this cohort are shown in Table 2. Bland-Altman plots showing agreement between devices for pRNFL and GCIPL Thicknesses are shown in Figure 3.

A conversion equation for pRNFL thickness between Cirrus and Spectralis SD-OCT was developed based upon 346 healthy control eyes that were scanned on both OCT devices on the same day, with repeated measures on at least on device, at a single site (NYU) using structural equation modeling. The conversion equation performed well when tested on an independent dataset for both healthy controls (n=95 eyes, R^2 = 0.85, LOOCV) and people with MS (n=37 eyes, R^2 = 0.91, LOOCV). The conversion equation for pRNFL is as follows (* symbol indicates multiplication):

$$[\text{Cirrus} = -5.0 + (1.0^{*}\text{Spectralis global pRMFL value})]$$

$$[\text{Spectralis} = 5.0 + (1.0^{*}\text{Cirrus global pRNFL value})]$$

The standard error for the equation was 0.02 and the overall SEM model had R^2=0.994. The 95% confidence interval (CI) for the beta coefficient was (0.96, 1.05), and for the intercept was (0.95, 9.00).

Similarly, for GCIPL, the conversion equation was developed on 228 healthy control eyes scanned consecutively on each device on the same day. The equation performed well in an independent dataset of healthy controls (n=22 eyes, R^2 = 0.933, LOOCV) and people

with MS (n=6 eyes, R^2 = 0.948, LOOCV), although the sample size may be too small to validate results. The conversion equation for GCIPL is as follows (* symbol indicates multiplication):

$$[\text{cirrus} = -4.5 + (0.9^{*}\text{spectralis global GCIPL value})]$$

$$[\text{Spectralis} = 5.0 + (1.1^{*}\text{Cirrus global GCIPL value})]$$

The standard error for the equation was 0.02 and the overall SEM model had R^2=0.996. The 95% confidence interval (CI) for the beta coefficient was (0.83, 0.93) and for the intercept was (−8.35, −0.58).

An example of utilizing the equation and the predictive error of the 95% CI would be if we used a value of 100 microns for Spectralis GCIPL. Using the conversion equation, Cirrus would equal 85.5 microns. If we consider the lowest extreme of the 95% CI (−8.35 intercept and 0.83 beta coefficient) and the highest (−0.58 intercept and 0.93 beta coefficient), we would have Cirrus = 74.65 or Cirrus = 92.2 microns. This would be a difference of 10.8% or 6.7% respectively from the predicted value of 85.5 microns using the equation.

Normative Data

Data from the whole cohort (n=540 healthy controls) showed a mean pRNFL thickness of 93.8 (SD 9.9) microns and a mean GCIPL thickness of 84.6 (SD 6.7) microns. Mean pRNFL and GCIPL thicknesses were consistent over decades 18–29, 30–39, and 40–49, and then showed a statistically significant decline for each subsequent decade (Table 1, Figure 4). Similar results were seen for each device individually before pooling data together. Device-specific normative values are shown in Supplementary Tables 2 **and** 3. Changepoint analyses showed a transition point at age 40 years for pRNFL and 37 years for GCIPL thicknesses (Figure 4). Age overall was associated with pRNFL decline at a rate of −1.31 microns per decade and a GCIPL decline at a rate of 1.05 microns per decade ($p<0.001$, statistical test). When considering age as a dichotomous variable (above or below age 40 years) based on changepoint analysis results, pRNFL decline was not associated with age below 40 years. However, there was an associated decline of 2.4 microns per decade above the age of 40 years ($p<0.001$, GEE models adjusting for sex, race, and country). Similarly, GCIPL had a faster decline above the age of 40 years (1.4 microns per decade, p=0.002, GEE models adjusting for sex, race, and country), and had no associated decline below age 40 years.

There were small differences in pRNFL thickness based on sex, with females having slightly higher thickness (by an average of 2.6 microns, p=0.003, GEE models adjusting for age, race/ethnicity, and country). There was no association between GCIPL thickness and sex. Likewise, there were no associations between race/ethnicity and pRNFL or GCIPL thicknesses (Table 1). Sensitivity analyses imputing missing race (n=63, 11.5%) and GCIPL thickness (n=140, 25.6%) showed similar results. Likewise, analyses separating SD-OCT

measures by device showed similar trends, suggesting that pooling of the data with the conversion equation did not potentially bias the results.

Discussion:

Results of this investigation demonstrate that a conversion factor is necessary when using two different SD-OCT devices clinically or in research studies. This study is unique since it pools together SD-OCT data on a large international multicenter study using a conversion factor. Furthermore, normative values for SD-OCT devices are presented in our investigations using a large diverse, multicenter, international cohort. We observed a decline in SD-OCT-measured pRNFL thickness after age 40 years and saw slightly thicker pRNFL values in females. SD-OCT has emerged as an important tool for detecting optic neuropathies and in capturing axonal and neuronal degeneration in MS. It is important to be able to compare SD-OCT measurements across different OCT platforms both clinically and in research studies. It is also critical to understand normative SD-OCT values based on age and sex.

The equation for conversion between Cirrus (C) and Spectralis (S) devices for pRNFL thickness ($C = -5.05 + S$) correlates well with the actual differences seen between the means of the groups (5 microns); its simplicity could make the equation highly useful for clinical practice and for observational research studies and clinical trials. The beta coefficient between the two devices was 1.0, suggesting the measurements are on the same scale, yet differing by 5 microns, with Spectralis being higher. While an equation for GCIPL was also developed, the small sample size of participants who had GCIPL measurements repeated on the Spectralis device was much smaller (33 eyes) than for pRNFL and the results may be underpowered. These findings, coupled with the variability in measurement area (median 14 (IQR 12.5–15.3) and segmentation algorithms, suggests this equation will need to be tested further to determine if it is generalizable to other studies. Importantly, our findings emphasize the need for a correction factor when comparing OCT measurements across platforms. To overcome variability between devices for GCIPL measures, a consistent segmentation algorithm could be used on both devices in lieu of a correction factor. However, pRNFL measurement is fairly standardized; the conversion equation may be useful in clinical trials, clinical practice, and other observational research studies.

In a previous study by Pierro et al, the pRNFL conversion factor between Cirrus and Spectralis was found to be Cirrus = 2.969 + 0.942*Heidelberg Spectralis. This is similar to our equation when considering numbers close to the mean for healthy controls. Both equations show Cirrus has a lower measurement than Spectralis at this scale. For example, a Spectralis measurement of 100 would equal a Cirrus measurement of 97.2 in Pierro's study, and 95.0 in our study. Our study had a much higher sample size (346 eyes vs 38 eyes), so our calculations may be more accurate.

In this large, multi-center international study, there were differences by sex only for pRNFL thickness; these were not observed for GCIPL thickness. A large population-based study in Germany of 7,868 Caucasian healthy control participants also found the pRNFL to be thicker in females (with variations depending on scanning distance from the optic

nerve and by quadrants), by 1 micron, while GCIPL was not evaluated(24). The Cirrus OCT Normative Database Study Group evaluated age and race differences for GCIPL on Cirrus OCT in 282 healthy controls participants and found no difference between males and females after adjusting for axial length; they also found no differences by race after adjusting for age, axial length and pRNFL thickness. These results are similar to those of the present study(25).

There were no differences between by race or ethnicity for either pRNFL or GCIPL measurements in our study cohort. Other reports have shown differences in retinal layer thicknesses between racial groups in both healthy control participants and in people with MS(15). A recent study of 31 African American (AA) and 61 Caucasian American (CA) healthy controls showed AAs had higher pRNFL thicknesses than CAs ($p=0.042$). There were no differences in GCIPL thicknesses in that study(16). Another study found that Asians had greater thicknesses for average pRNFL(26). The Cirrus OCT Normative Database Study Group found thinner pRNFL values in Europeans compared to Hispanics and Asians(25). The sample sizes for racial/ethnic groups in our study may have been too small to detect a difference. The potential differences in pRNFL or GCIPL measurements will need to be examined further and in larger cohorts.

Overall pRNFL and GCIPL thickness for the whole cohort are comparable to other studies(27, 28). A decline in pRNFL and GCIPL thickness, with a faster rate of thinning beyond age 40 years, was seen in our present study cohort. Other studies have shown declines in retinal thickness over-time in aging populations. A study of disease-free controls and MS participants found an average decline of 0.49 microns in pRNFL thickness over 3 years in the healthy control cohort; this is equivalent to a decline of 1.63 microns per decade(28). This study did not account for a faster decline after the age of 40 years, but results are similar to the overall decline found in our study of 1.31 microns per year. A study of normative values in an Asian Indian population showed a similar rate for decline in global pRNFL thickness (1.57 microns per decade)(29). Peripapillary RNFL thinning has been associated with brain atrophy in cognitively normal older adults,(30, 31) and, thus, may be a normal characteristic of aging.

Limitations of this study include that since this is not a population-based study, further evaluation of our conversion equations will be helpful to confirm generalizability. The equations developed in this study are applicable only to the Cirrus HD-OCT or Spectralis device and not interchangeable with other devices. Methods used in the analysis can be applied to develop equations across other OCT devices.

Another limitation includes some missing data for race/ethnicity and for GCIPL thickness. A sensitivity analysis, imputing race/ethnicity and GCIPL thickness, was performed and produced similar results; therefore, it is less likely this missing data created biases in the analysis. Race/ethnicity were self-reported for this study which can introduce some error. Furthermore, race and ethnicity are defined differently in the United States compared to other international sites. As such, race/ethnicity data collected from outside of the U.S. was translated as best as possible to the U.S. categories, which may introduce some measurement

error. However, this error is expected to be small and not likely to bias the data, particularly since almost all of the non-US participants were classified as Caucasian.

Lastly, there is limited clinical evaluations in the healthy control participants; these participants have self-reported that they have no known ophthalmological or neurological diseases. No formal ophthalmic assessment or measurement of intraocular pressure (IOP) was performed in most participants. One subset of the healthy control participants at NYU (n=74) did undergo clinical evaluation. Another subset of participants (n=139) completed vision-specific quality of life questionnaires (25-Item National Eye Institute Visual Functioning Questionnaire [NEI-VFQ-25]). The scores for these questionnaires were in a range that is consistent with self-reported healthy control status. We, therefore, would not expect a significant amount of bias to be introduced from self-reporting. Ocular axial length has been associated with reduced retinal thickness(32) and with sex,(25) but axial length was not measured in this study. However, in a study that was used to develop the Cirrus normative database, refractive error and axial length explained less than 2% of variability for the model(33). While it is possible that axial length could explain variations in sex differences, not having this measurement in the model is not likely to add significant degrees of bias. Since participants with high-contrast visual acuities worse than 20/40 Snellen equivalent were excluded, and participants self-reported no history of neurological or ophthalmological disease, our control cohort may be healthier than the general population. Results when evaluating a typical aging population, including those with other ocular pathologies including diabetes, high myopia, and macular degeneration, may show varied data for pRNFL and GCIPL thickness.

The evolution of SD-OCT presents a unique opportunity to evaluate for optic nerve degeneration in people with MS. Measurements from different devices are not necessarily interchangeable due to differences in segmentation algorithms and acquisition protocols that introduce systematic biases between devices. This may complicate our ability to track disease progression over time if different devices are used. However, a conversion equation or correction factor, as developed in the present investigation, can allow for pooling of data acquired on different devices for research studies. This can also facilitate comparisons of results from different OCT devices. The equations will be helpful, for example, if a patient was scanned clinically on one OCT device, and then scanned on a different device subsequently at the next follow-up visit. The availability of normative data by age decade facilitates the evaluation of normal SD-OCT thickness values and age-specific normative data by decade should be considered when assessing for retinal thinning. Rates of decline over time in cohorts of healthy controls may help to determine if an MS patient, by comparison, has an abnormal rate of retinal thinning. Results from the present study will increase the utility of OCT as a diagnostic tool for optic nerve degeneration in MS in particular, and for other neuro-ophthalmologic disorders in general.

Supplementary Material

Refer to Web version on PubMed Central for supplementary material.

Acknowledgments

Financial Support: This study was supported in part by the NYU School of Medicine.

References

1. Nolan RC, Akhand O, Rizzo JR, Galetta SL, Balcer LJ. Evolution of Visual Outcomes in Clinical Trials for Multiple Sclerosis Disease-Modifying Therapies. Journal of neuro-ophthalmology : the official journal of the North American Neuro-Ophthalmology Society. 2018;38(2):202–9. [PubMed: 29750734]
2. Bhargava P, Lang A, Al-Louzi O, Carass A, Prince J, Calabresi PA, et al. Applying an Open-Source Segmentation Algorithm to Different OCT Devices in Multiple Sclerosis Patients and Healthy Controls: Implications for Clinical Trials. Multiple sclerosis international. 2015;2015:136295.
3. Pierro L, Gagliardi M, Iuliano L, Ambrosi A, Bandello F. Retinal Nerve Fiber Layer Thickness Reproducibility Using Seven Different OCT Instruments. Investigative Opthalmology & Visual Science. 2012;53(9).
4. Miller M, Zemon V, Nolan-Kenney R, Balcer LJ, Goff DC, Worthington M, et al. Optical coherence tomography of the retina in schizophrenia: Inter-device agreement and relations with perceptual function. Schizophrenia Research. 2020.
5. Watson GM, Keltner JL, Chin EK, Harvey D, Nguyen A, Park SS. Comparison of retinal nerve fiber layer and central macular thickness measurements among five different optical coherence tomography instruments in patients with multiple sclerosis and optic neuritis. Journal of neuro-ophthalmology : the official journal of the North American Neuro-Ophthalmology Society. 2011;31(2):110–6. [PubMed: 21131852]
6. Lange AP, Sadjadi R, Costello F, Guber I, Traboulsee AL. Reproducibility of retinal nerve fiber layer measurements with manual and automated centration in healthy subjects using spectralis spectral-domain optical coherence tomography. ISRN Ophthalmol. 2012;2012:860819.
7. Oberwahrenbrock T, Weinhold M, Mikolajczak J, Zimmermann H, Paul F, Beckers I, et al. Reliability of Intra-Retinal Layer Thickness Estimates. PloS one. 2015;10(9):e0137316.
8. Syc SB, Warner CV, Hiremath GS, Farrell SK, Ratchford JN, Conger A, et al. Reproducibility of high-resolution optical coherence tomography in multiple sclerosis. Multiple sclerosis (Houndmills, Basingstoke, England). 2010;16(7):829–39. [PubMed: 20530512]
9. Oberwahrenbrock T, Traber GL, Lukas S, Gabilondo I, Nolan R, Songster C, et al. Multicenter reliability of semiautomatic retinal layer segmentation using OCT. Neurol Neuroimmunol Neuroinflamm. 2018;5(3):e449. [PubMed: 29552598]
10. Warner CV, Syc SB, Stankiewicz AM, Hiremath G, Farrell SK, Crainiceanu CM, et al. The impact of utilizing different optical coherence tomography devices for clinical purposes and in multiple sclerosis trials. PloS one. 2011;6(8):e22947.
11. Buchser NM, Wollstein G, Ishikawa H, Bilonick RA, Ling Y, Folio LS, et al. Comparison of retinal nerve fiber layer thickness measurement bias and imprecision across three spectral-domain optical coherence tomography devices. Invest Ophthalmol Vis Sci. 2012;53(7):3742–7. [PubMed: 22538423]
12. Koh VT, Tham Y-C, Cheung CY, Wong W-L, Baskaran M, Saw S-M, et al. Determinants of Ganglion Cell–Inner Plexiform Layer Thickness Measured by High-Definition Optical Coherence Tomography. Investigative Opthalmology & Visual Science. 2012;53(9).
13. Motamedi S, Gawlik K, Ayadi N, Zimmermann HG, Asseyer S, Bereuter C, et al. Normative Data and Minimally Detectable Change for Inner Retinal Layer Thicknesses Using a Semi-automated OCT Image Segmentation Pipeline. Front Neurol. 2019;10:1117. [PubMed: 31824393]
14. Budenz DL, Anderson DR, Varma R, Schuman J, Cantor L, Savell J, et al. Determinants of normal retinal nerve fiber layer thickness measured by Stratus OCT. Ophthalmology. 2007;114(6):1046–52. [PubMed: 17210181]
15. Kimbrough DJ, Sotirchos ES, Wilson JA, Al-Louzi O, Conger A, Conger D, et al. Retinal damage and vision loss in African American multiple sclerosis patients. Ann Neurol. 2015;77(2):228–36. [PubMed: 25382184]

16. Caldito NG, Saidha S, Sotirchos ES, Dewey BE, Cowley NJ, Glaister J, et al. Brain and retinal atrophy in African-Americans versus Caucasian-Americans with multiple sclerosis: a longitudinal study. Brain. 2018;141(11):3115–29. [PubMed: 30312381]
17. Balcer LJ, Balk LJ, Brandt AU, Calabresi PA, Martinez-Lapiscina EH, Nolan RC, et al. The International Multiple Sclerosis Visual System Consortium: Advancing Visual System Research in Multiple Sclerosis. Journal of neuro-ophthalmology : the official journal of the North American Neuro-Ophthalmology Society. 2018;38(4):494–501. [PubMed: 30418332]
18. Martinez-Lapiscina EH, Arnow S, Wilson JA, Saidha S, Preiningerova JL, Oberwahrenbrock T, et al. Retinal thickness measured with optical coherence tomography and risk of disability worsening in multiple sclerosis: a cohort study. The Lancet Neurology. 2016;15(6):574–84. [PubMed: 27011339]
19. Cruz-Herranz A, Balk LJ, Oberwahrenbrock T, Saidha S, Martinez-Lapiscina EH, Lagreze WA, et al. The APOSTEL recommendations for reporting quantitative optical coherence tomography studies. Neurology. 2016;86(24):2303–9. [PubMed: 27225223]
20. Aytulun A, Cruz-Herranz A, Aktas O, Balcer LJ, Balk L, Barboni P, et al. APOSTEL 2.0 Recommendations for Reporting Quantitative Optical Coherence Tomography Studies. Neurology. 2021;97(2):68–79. [PubMed: 33910937]
21. Nolan-Kenney RC, Liu M, Akhand O, Calabresi PA, Paul F, Petzold A, et al. Optimal intereye difference thresholds by optical coherence tomography in multiple sclerosis: An international study. Ann Neurol. 2019;85(5):618–29. [PubMed: 30851125]
22. Tewarie P, Balk L, Costello F, Green A, Martin R, Schippling S, et al. The OSCAR-IB consensus criteria for retinal OCT quality assessment. PLoS One. 2012;7(4):e34823.
23. Bollen KA. Structural equations with latent variables. New York: Wiley; 1989. xiv, 514 p. p.
24. Li D, Rauscher FG, Choi EY, Wang M, Baniasadi N, Wirkner K, et al. Sex-Specific Differences in Circumpapillary Retinal Nerve Fiber Layer Thickness. Ophthalmology. 2020;127(3):357–68. [PubMed: 31732228]
25. Mwanza JC, Durbin MK, Budenz DL, Girkin CA, Leung CK, Liebmann JM, et al. Profile and predictors of normal ganglion cell-inner plexiform layer thickness measured with frequency-domain optical coherence tomography. Invest Ophthalmol Vis Sci. 2011;52(11):7872–9. [PubMed: 21873658]
26. Poon LY, Antar H, Tsikata E, Guo R, Papadogeorgou G, Freeman M, et al. Effects of Age, Race, and Ethnicity on the Optic Nerve and Peripapillary Region Using Spectral-Domain OCT 3D Volume Scans. Transl Vis Sci Technol. 2018;7(6):12.
27. Alasil T, Wang K, Keane PA, Lee H, Baniasadi N, de Boer JF, et al. Analysis of normal retinal nerve fiber layer thickness by age, sex, and race using spectral domain optical coherence tomography. J Glaucoma. 2013;22(7):532–41. [PubMed: 22549477]
28. Talman LS, Bisker ER, Sackel DJ, Long DA Jr., Galetta KM, Ratchford JN, et al. Longitudinal study of vision and retinal nerve fiber layer thickness in multiple sclerosis. Ann Neurol. 2010;67(6):749–60. [PubMed: 20517936]
29. Appukuttan B, Giridhar A, Gopalakrishnan M, Sivaprasad S. Normative spectral domain optical coherence tomography data on macular and retinal nerve fiber layer thickness in Indians. Indian J Ophthalmol. 2014;62(3):316–21. [PubMed: 24008793]
30. Shi Z, Cao X, Hu J, Jiang L, Mei X, Zheng H, et al. Retinal nerve fiber layer thickness is associated with hippocampus and lingual gyrus volumes in nondemented older adults. Prog Neuropsychopharmacol Biol Psychiatry. 2020;99:109824.
31. Shi Z, Zheng H, Hu J, Jiang L, Cao X, Chen Y, et al. Retinal Nerve Fiber Layer Thinning Is Associated With Brain Atrophy: A Longitudinal Study in Nondemented Older Adults. Front Aging Neurosci. 2019;11:69. [PubMed: 31031615]
32. Jonas JB, Xu L, Wei WB, Pan Z, Yang H, Holbach L, et al. Retinal Thickness and Axial Length. Invest Ophthalmol Vis Sci. 2016;57(4):1791–7. [PubMed: 27074383]
33. Meditec CZ. 501(k) Summary. 2015.

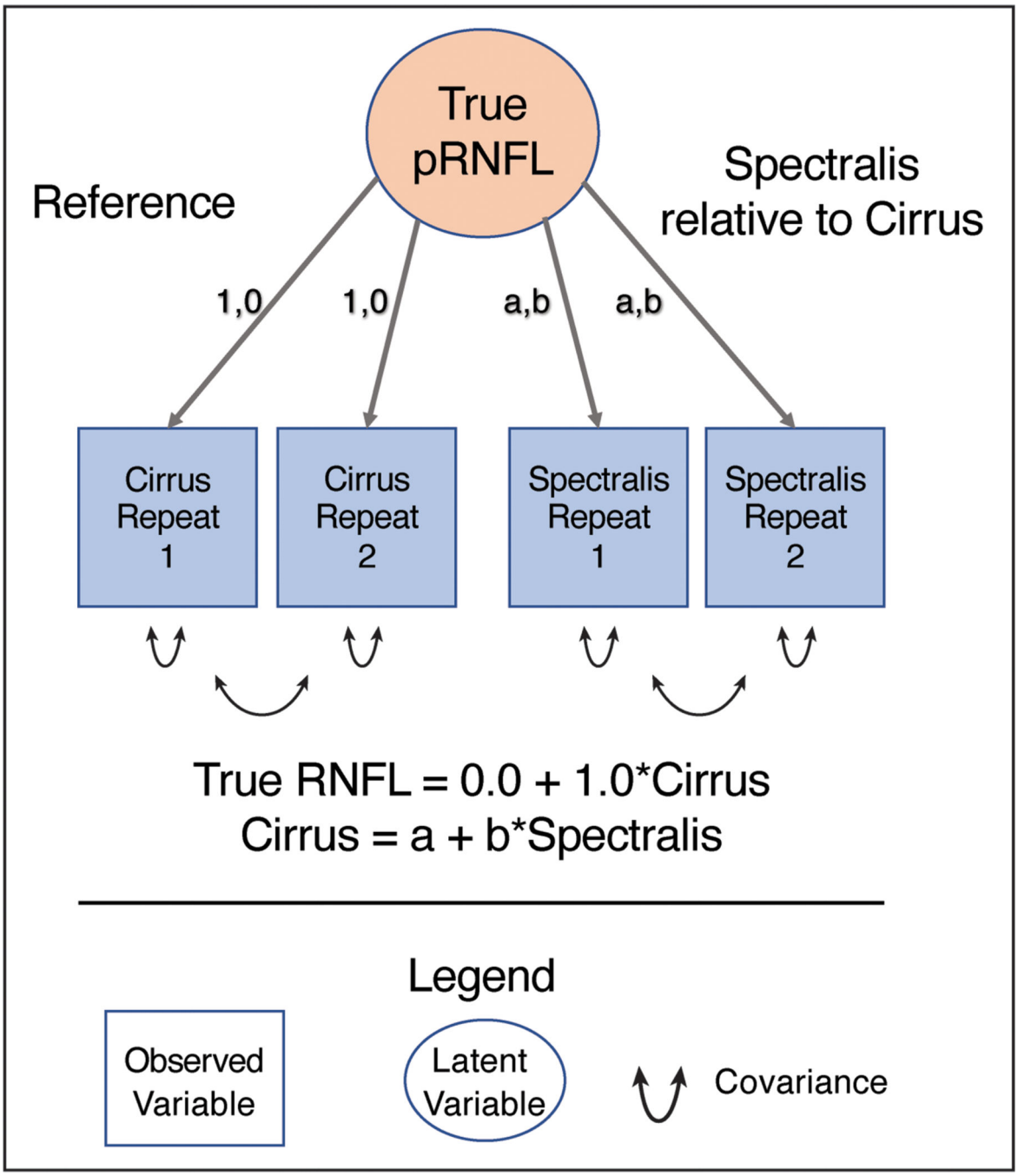

Figure 1: SEM model.

The path diagram illustrates the structural equation model (SEM) that describes the relationship of the repeated pRNFL measurements for each SD-OCT device with the unknown true global pRNFL thickness values. Cirrus is set as the reference value for comparison to Spectralis.

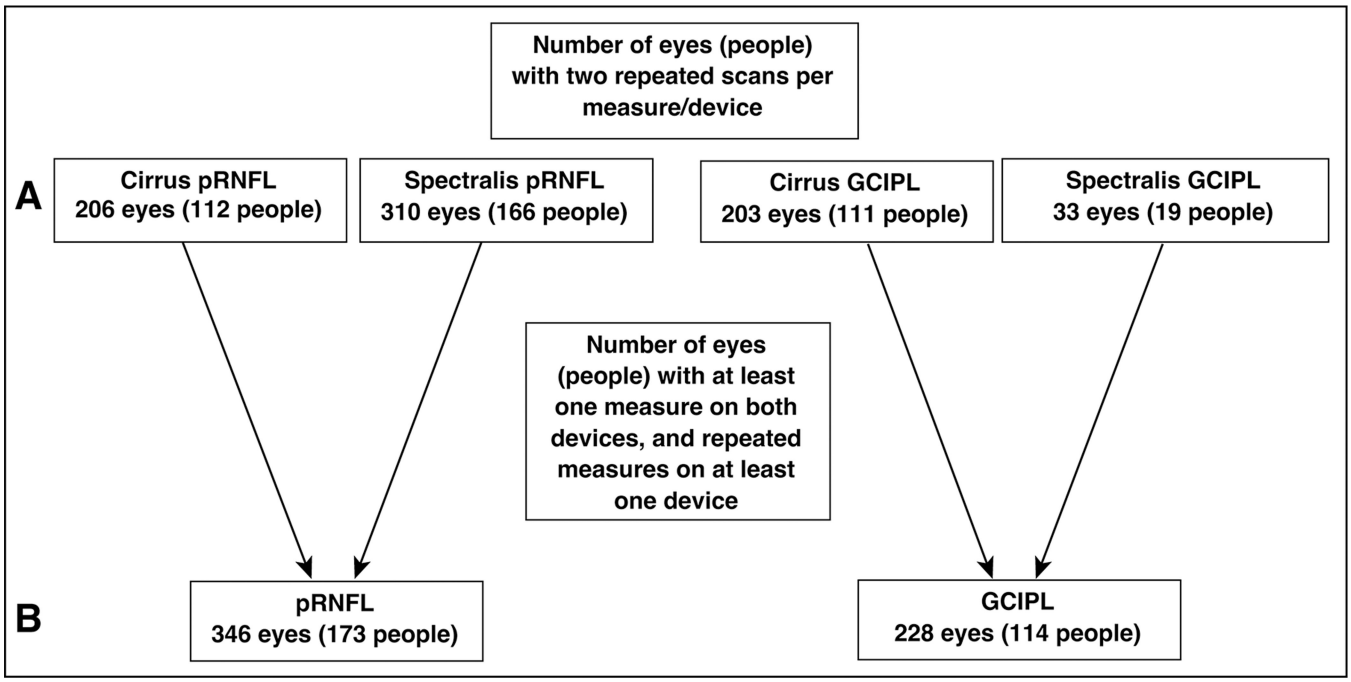

Figure 2. Flow chart of scans used in reproducibility and SEM analyses.

The number of eyes (people) who were scanned for each individual measure on each device repeated twice on the same day is depicted in line A. These scans were used to determine reproducibility results shown in Table 2. Line B shows the number of eyes (people) who were used in the SEM model. These people had at least one measure on both devices, and repeated measures on at least one device.

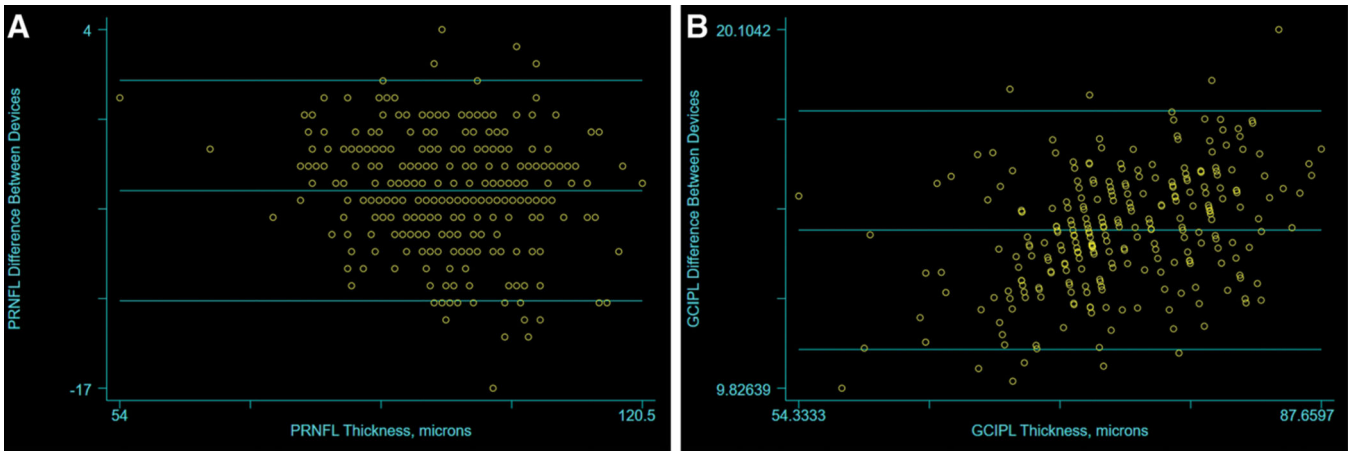

Figure 3. Bland-Altman Plots.

A) Bland-Altman plot for pRNFL thickness showing agreement between devices. The y-axis shows the difference in measurement between Cirrus pRNFL and Spectralis pRNFL thickness. The x-axis shows the pRNFL thickness. B) Bland-Altman plot for GCIPL thickness.

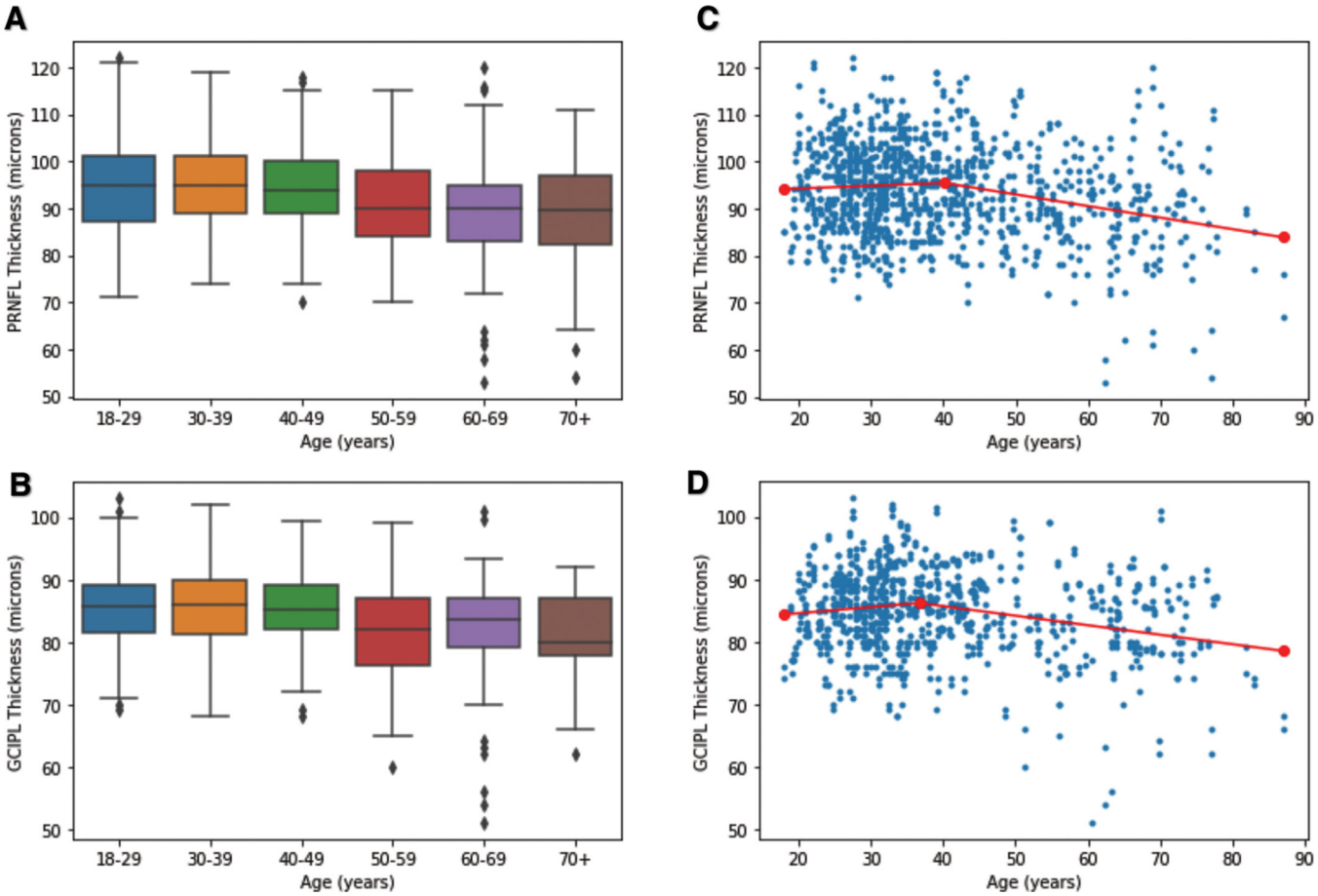

Figure 4.

Boxplot for pRNFL thickness by age (A) and GCIPL thickness by age (B). Scatterplot with changepoint analysis for pRNFL (C) and GCIPL (D).

J Neuroophthalmol. Author manuscript; available in PMC 2023 December 01.

Table 1.

Demographic and SD-OCT summary statistics and GEE results for healthy control cohort

		pRNFL (n=546)			GCIPL (n=406)		
	Frequency (Number/percent)	**Mean (SE)***	**Beta Coefficient (95% CI)**	**p-value****	**Mean (SE)***	**Beta Coefficient (95% CI)**	**p-value****
Age, years							
18–29	165 (30.2)	94.8 (0.7)	Reference	Reference	85.2 (0.5)	Reference	Reference
30–39	179 (32.8)	94.9 (0.7)	−0.41 (−2.51, 1.70)	0.705	85.6 (0.5)	−0.31 (−1.68, 1.06)	0.659
40–49	81 (14.8)	94.4 (1.0)	−0.65 (−3.31, 2.00)	0.630	85.4 (0.7)	−0.51 (−2.19, 1.17)	0.550
50–59	50 (9.2)	91.2 (1.3)	−2.15 (−5.35, 1.04)	0.187	82.0 (1.4)	−2.58 (−4.71, −0.44)	0.018
60–69	48 (8.8)	89.1 (1.7)	−6.11 (−9.21, −3.01)	<0.001	82.2 (1.2)	−4.81 (−6.70, −2.92)	<0.001
70+	23 (4.2)	88.2 (2.3)	−6.65 (−10.68, −2.63)	0.001	80.8 (1.5)	−4.05 (−6.44, −1.66)	0.001
Sex							
Male	247 (45.2)	92.5 (0.6)	Reference	Reference	84.4 (0.4)	Reference	Reference
Female	303 (54.9)	94.6 (0.5)	2.60 (0.91, 4.29)	0.003	84.8 (0.4)	−0.32 (−1.41, 0.77)	0.562
Race							
Caucasian	413 (75.6)	93.6 (0.5)	Reference	Reference	85.3 (0.4)	Reference	Reference
Hispanic	11 (2.0)	97.6 (3.1)	3.89 (−1.62, 9.41)	0.166	82.5 (2.2)	−0.79 (−4.11, 2.53)	0.640
African American	22 (4.0)	94.0 (2.0)	1.55 (−2.49, 5.59)	0.453	81.8 (1.4)	0.47 (−2.09, 3.03)	0.718
Asian or Pacific Islander	29 (5.3)	92.3 (1.5)	−1.18 (−4.76, 2.41)	0.520	83.2 (1.6)	0.83 (−1.97, 3.63)	0.560
Other	8 (1.5)	90.6 (0.9)	−1.70 (−8.16, 4.76)	0.607	79.9 (1.4)	−1.28 (−4.49, 1.93)	0.434
Missing	63 (11.5)	94.2 (1.1)	–	–	83.1 (0.8)	–	–
Country							
Germany	54 (9.9)	92.7 (1.2)	Reference	Reference	84.8 (0.5)	Reference	Reference
Holland	19 (3.5)	87.1 (1.8)	−5.10 (−10.06, −0.13)	0.044	–	–	–
Kuwait	38 (7.0)	96.0 (1.0)	2.50 (−1.29, 6.28)	0.196	83.7 (0.6)	−2.05 (−4.61, 0.50)	0.115
Spain	108 (19.8)	94.6 (0.9)	2.97 (−0.01, 5.95)	0.051	88.6 (0.4)	4.12 (1.94, 6.30)	<0.001
Switzerland	33 (6.0)	99.0 (1.6)	5.53 (1.58, 9.49)	0.006	93.3 (0.7)	7.48 (4.84, 10.12)	<0.001
United States	294 (53.9)	93.0 (0.6)	0.46 (−2.37, 3.30)	0.748	81.9 (0.4)	−3.42 (−5.58, −1.25)	0.002

pRNFL = peripapillary retinal nerve fiber lyaerl GCIPL = ganglion cell+inner plexiform layer, SE = standard error, GEE = generatlized estimating equation

* Means and standard errors calculated using linear mixed effects models accounting for clustering of two eyes per subject

** Beta estimates and p-values estimated using GEE models accounting for clustering of two eyes per subject

Table 2.

Reproducibility of OCT measurements for healthy control cohort at single site (NYU) with repeated measures

	Cirrus pRNFL	Spectralis pRNFL	Cirrus GCIPL	Spectralis GCIPL
Number with repeated measures, eyes (people)	206 (112)	310 (166)	203 (111)	33 (19)
Difference Between Repeated Measures, microns, median (IQR/range)	1 (0–2 (0–8)	1 (0–2 (0–6)	0 (0–1 (0–6)	0.4 (0.2–0.7) 0.0–2.7)
ICC (repeated measures)	0.998	0.996	0.995	0.997
CoV (repeated Measures)	2.07%	1.48%	1.24%	1.16%
Difference between devices, microns, median (IQR/ range)	5 (3–7) (0–17) *		14 (12.5–15.3) (5.0–18.6) **	

* n=439 eyes (224) people had at least one pRNFL measurements on both Spectralis and Cirrus devices.

** n=216 eyes (109) people had at least one GCIPL measurements on both Spectralis and Cirrus devices.